Homozygous hypomorphic BRCA2 variant in primary ovarian insufficiency without cancer or Fanconi anaemia trait

Sandrine Caburet, Abdelkader Heddar, Elodie Dardillac, Héléne Creux, Marie Lambert, Sébastien Messiaen, Sophie Tourpin, Gabriel Livera, Bernard Lopez, Micheline Misrahi

A homozygous hypomorphic *BRCA2* variant causes primary ovarian insufficiency without cancer or Fanconi anemia traits.

Sandrine Caburet[1,#], Abdelkader Heddar[2,#], Elodie Dardillac[3,4,#], Helene Creux[5], Marie Lambert[5], Sébastien Messiaen[6], Sophie Tourpin[6], Gabriel Livera[6], Bernard S. Lopez[3,4,*], Micheline Misrahi[2,*]

[1] Université de Paris, Institut Jacques Monod, CNRS UMR7592, F-75013 Paris, France.

[2] Faculté de Médecine, Universités Paris-Sud-Paris-Saclay, Hôpital Bicêtre, 94275, Le Kremlin Bicêtre, France.

[3] Institut Cochin, INSERM U1016, UMR 8104 CNRS, Université de Paris, 75014 Paris, France. Team labeled by "Ligue Nationale contre le cancer, Ligue 2017".

[4] CNRS UMR 8200, Institut de Cancérologie Gustave-Roussy, Université Paris-Saclay, Villejuif, France.

[5] Service de Gynécologie et Médecine de la Reproduction, CHU de Bordeaux, 33000, France.

[6] UMR Stabilité Génétique, Cellules Souches et Radiations, Université de Paris, Université Paris-Saclay, CEA/DRF/iRCM/SDRR/LDG, 18 route du Panorama, Fontenay aux Roses, F-92265, France.

[#] These authors contributed equally to this work.

* Corresponding author: micheline.misrahi@aphp.fr.

* Corresponding author: bernard.lopez@inserm.fr.

Running title: Mutant BRCA2 in isolated ovarian insufficiency.

ABSTRACT

Primary Ovarian insufficiency (POI) affects 1% of women under forty. We studied a patient with a non-syndromic POI, from a consanguineous Turkish family. Exome sequencing identified a homozygous missense variant c.8524C>T/p.R2842C in *BRCA2*. BRCA2 is a major player in homologous recombination (HR). BRCA2 deficiency induces cancer predisposition and Fanconi Anemia (FA). Remarkably, neither the patient nor her family exhibit somatic pathologies. The patient's somatic cells presented intermediate levels of chromosomal breaks, cell proliferation and radiation-induced RAD51 foci formation when compared to controls, the heterozygous mother's and FA cells. R2842C-BRCA2 partially complemented BRCA2 depletion for double-strand break-induced HR. The residual HR function in patient's cells could explain the absence of somatic pathology. BRCA2 is expressed in human fetal ovaries in pachytene stage oocytes, when meiotic HR occurs. This study has a major impact on the understanding of genome maintenance in somatic and meiotic cells and on the management of POI patients.

Keywords: BRCA2 / mutation / cancer / Fanconi anemia / Primary ovarian insufficiency / meiosis.

INTRODUCTION

Primary ovarian insufficiency (POI) is a public health issue affecting ~1% of women under 40 years, and is clinically heterogeneous with isolated or syndromic forms (Huhtaniemi et al., 2018). Most cases are idiopathic but an increasing number of genetic causes have been recently identified, especially mutations in genes involved in DNA repair and recombination (AlAsiri et al., 2015; Fouquet et al., 2017; Wood-Trageser et al., 2014).

DNA repair and recombination are essential for genome maintenance. The DNA damage response (DDR) coordinates a network of pathways insuring faithful transmission of genetic material. Consistently, defects in the DDR result in genome instability associated with developmental anomalies and cancer predisposition (Hoeijmakers, 2009).Homologous recombination (HR), an evolutionary conserved process essential to genome stability and cell viability, plays crucial roles in DNA double strand break (DSB) repair in somatic and meiotic cells.

In mammals, BRCA2 binds damaged DNA and loads the pivotal HR player RAD51, which then promotes DNA homology search. Therefore, cells defective in RAD51 or BRCA2 are thus defective in mitotic HR (Lambert and Lopez, 2000; Moynahan et al., 2001). Heterozygous *BRCA2* mutations increase susceptibility to breast and ovarian cancers, whereas severe bi-allelic defects in *RAD51* (*FANCR*) or *BRCA2 (FANCD1)* lead to Fanconi anemia (FA) syndrome (Tsui and Crismani, 2019). In particular, *FANCD1* syndrome associates developmental defects, genetic instability, bone marrow failure and cancer predisposition, with cancer developing in the first decade of life, and death before puberty (Meyer et al., 2014) . The role of BRCA2 in RAD51 loading in mitotic HR makes it a strong candidate for an involvement in meiotic HR, but this remains to be formally established. Indeed, the severe phenotypes of bi-allelic inactivation of BRCA2 in humans and the early embryonic lethality resulting from germ-line inactivation of this essential gene in animal models hampered meiosis analysis and

compromised the study of the putative functions of BRCA2 in gametogenesis (Ludwig et al., 1997; Sharan et al., 1997; Tsuzuki et al., 1996).

We describe here an adult patient carrying a homozygous missense mutation in *BRCA2* with isolated POI, but without cancer nor FA traits in the patient or her family. We demonstrate that the mutated R2842C-BRCA2 retains a lower but significant residual function when compared to wild-type (WT)-BRCA2. Consistently, the patient's cells exhibit intermediate levels in chromosomal breaks, cell proliferation and ionizing radiation-induced RAD51 foci formation when compared to controls, a FANCD1 patient's or the heterozygous mother's cells. This residual HR in somatic cells could explain the absence of *in vivo* somatic pathologies. BRCA2 is a major cancer susceptibility gene and our finding will have a strong impact on the genetic counselling and management of patients with POI and their relatives.

RESULTS

Case report

The proposita was born to consanguineous Turkish parents (Figure 1). At 13 years, she had two vaginal bleedings followed by primo-secondary amenorrhea. She had normal pilosity, breast development and external genitalia. Several hormonal assays confirmed POI and pelvic ultrasonographical studies showed small ovaries with no or very few follicles (Table 1). Blood counts, liver and thyroid balances were normal. Thyroid auto-antibodies were undetectable. Bone densitometry at 30 years showed a marked osteopenia (T score = -2.3). She is presently 41 years old, displays normal blood assays and no other clinical sign. The karyotype is 46, XX and FMR1 premutation screening was negative. After two egg-donation procedures, she had two pregnancies with four healthy children.

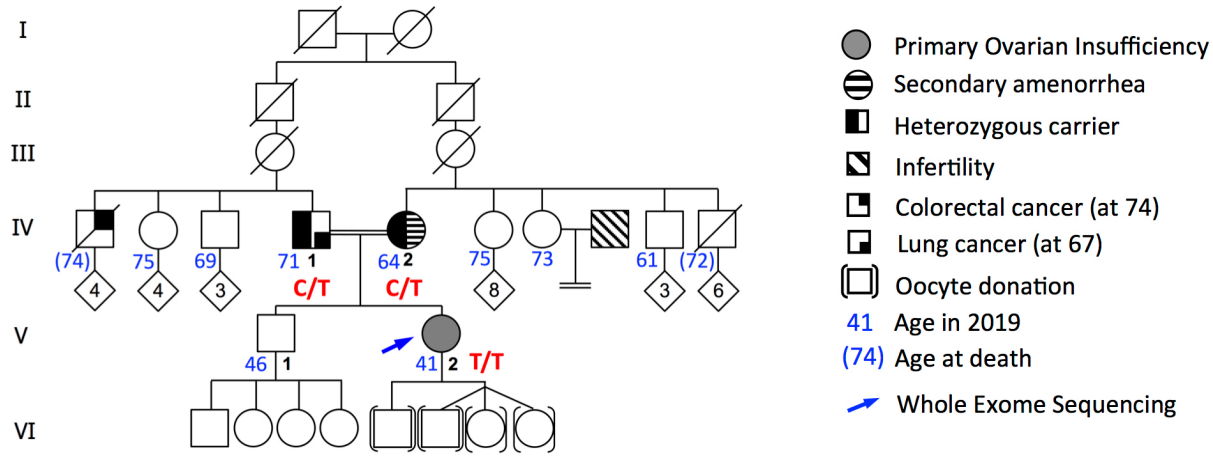

Figure 1: Pedigree of the Turkish family. Double lines indicate consanguineous union. The proband (blue arrow) was analysed by WES. The genotypes for the mutated codon of *BRCA2* are indicated in red.

The patient and family members have a normal stature, normal head circumferences with no abnormality in skin pigmentation, skeletal development or dysmorphia (Table 1). There was no familial history of infertility or other diseases. The mother married at the age of 15 and had two pregnancies at 18 (a boy) and 22 years (the proposita). This is in line with a delayed conception followed by secondary amenorrhea at the age of 33, not investigated in Turkey. She is obese with a BMI of 38. In order to rule out other genetic causes that could explain her subfertility, we performed a targeted NGS (see supplementary information). The brother had one healthy son (17 years) and 3 healthy daughters aged 15, 13 (both with normal puberty) and 8 years. The 71 years-old father, a heavy smoker, had a lung cancer at the age of 67 years, treated by radiotherapy and chemotherapy. A paternal uncle developed a colorectal cancer at the age of 74 years and died few months later. Six other paternal and maternal uncles and aunts are 61 to 75 years old and have no history of cancer or infertility.

Case	Menstrual cycles	Age at evaluation (years)	BMI (height cm/ weight kg)	Head circumference cm (SD)	(R/L) Ovarian Volume mm^3	(R/L) Follicle number	FSH IU/l	LH IU/l	E2 nmol/l	AMH ng/ml	InhB ng/l	T nmol/l	PRL ng/ml	TSH mU/l
Index	Primo-Secondary amenorrhea (13 years)	30	23 (156/55)	55.5 (0)	21/17 0.9/0.5	2/0	85	16.7	0.04			0.5	17.5	1.45
		32			19/17	0/0	113	36.5	0.08			0.6	29.5	1.34
		39	24 (156/58)				111	26.5	0.09	0.03	< 8	1.43	4.6	1.66
Mother	Secondary amenorrhea (33 years)	63	38 (155/90)	56 (0)	**Normal ranges**	Follicular phase	2.9-12	1.5-8	0.06-0.54	2.2 - 6.8	10 - 320	0.4 - 2	0.7 - 25	0.3 - 4.2
						Ovulatory phase	6.3-24	9.6-80	0.16-0.78					
Father		70	17 (170/50)	55 (0)		Luteal phase	1.5-7	0.2-6.5	0.34-2.1					
Brother		45	28 (171/80)	57 (0)		Menopause	17-95	8-33	≤0.2					

Table 1: Clinical and biological studies of the proband and relatives.

BMI: body mass index; SD: deviation compared to standards; R: Right; L: Left; FSH: Follicle-stimulating hormone; LH: Luteinizing hormone; E2: estradiol; AMH: anti-Müllerian hormone; InhB: inhibine B; T: testosterone; PRL: prolactin; TSH: thyroid-stimulating hormone.

Whole-exome sequencing identified a homozygous missense variant in the DNA-binding domain of *BRCA2*

The patient was studied by whole-exome sequencing (WES). Familial consanguinity suggested an autosomal recessive inheritance pattern. The variants were therefore filtered on the basis of their homozygosity in the patient, their absence in unrelated fertile in-house controls and a minor allele frequency (MAF) below 0.01 in all available databases. Further filtering on available functional data for a possible role in fertility revealed the missense variant rs80359104, NM_000059.3: c.8524C>T (p.R2842C), located in exon 20 of *BRCA2* (Figure 2A, Figure 2–figure supplement 1 and Figure 2–figure supplement 2). The variant is very rare and presents only at the heterozygous state in 3 out of 138342 individuals without known phenotype (MAF 1.10^{-5}) in the non-cancer GnomAD subset. It is absent in the Greater Middle East Variome database dedicated to Middle Eastern populations. It is predicted to be pathogenic by 16 of 17 predictive softwares (Figure 2–figure supplement 3).

The variant changes a strictly-conserved aminoacid (aa) at the base of the Tower part of the BRCA2 DNA-binding domain, in close proximity to the groove that binds single-stranded DNA (ssDNA) (Figure 2B and Figure 2–figure supplement 4). This C-terminal domain is essential for appropriate binding of BRCA2 to ssDNA (Yang et al., 2002).

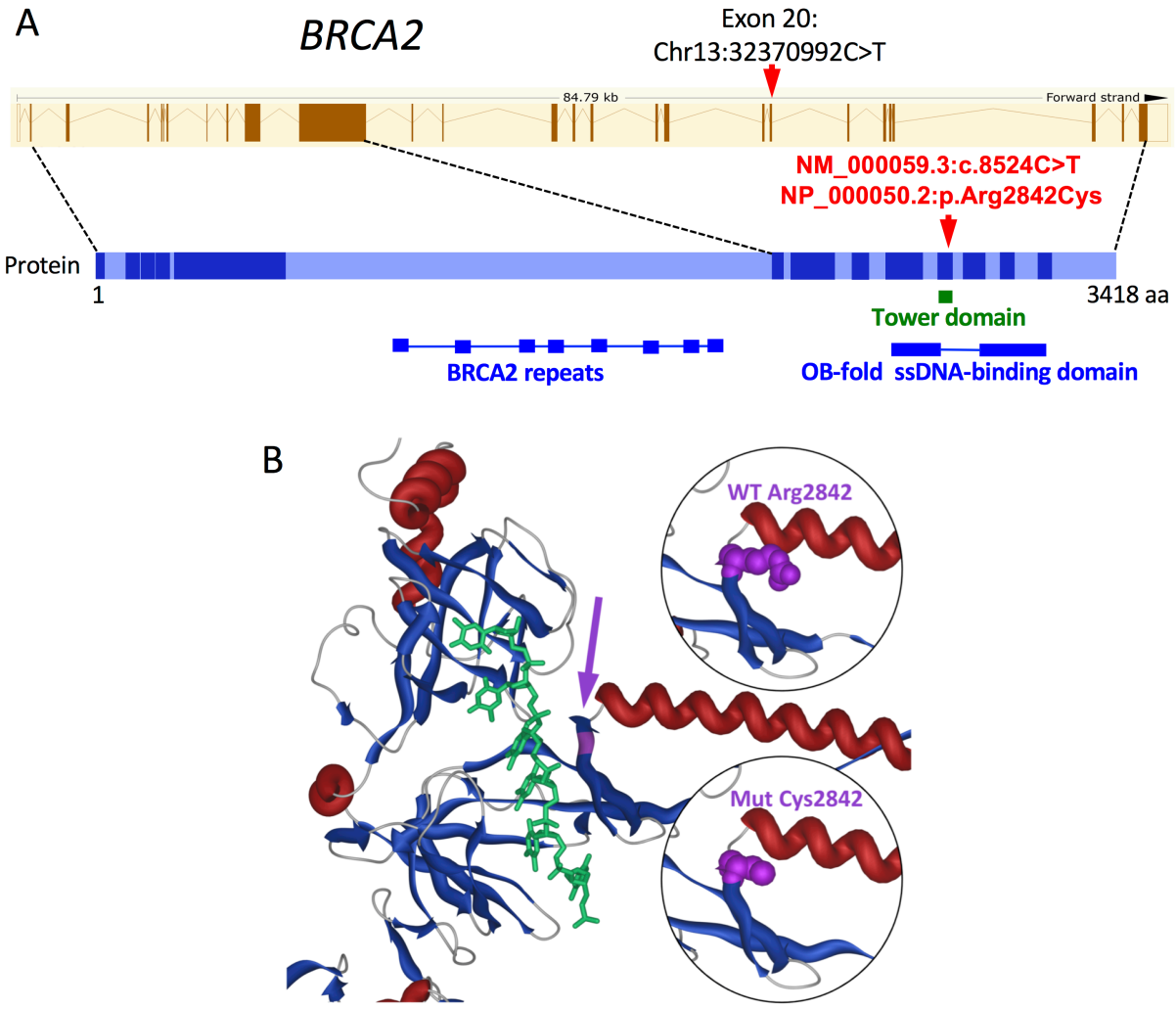

Figure 2: Mutation of *BRCA2* in a POI patient without FA trait. A. Position of the variant in *BRCA2* gene and protein. The structure of the normal protein for the longest isoform of 3418 residues is shown below the genomic structure with the coding exons as coloured bars (Ensembl, reference transcript ENST00000544455.5). The mutation (red arrow) lies at the very end of exon 20, which encodes 48 aminoacids (aa) encompassing the Tower domain at the center of the OB-fold ssDNA-binding domain (oligonucleotide/oligosaccharide -Binding single-strand DNA-binding domain). **B.** Partial view of the 3D model of the BRCA2 C-terminal domain (alpha-helices in red, beta-sheets in blue). The mutated position (purple) is located near the

ssDNA (green), at the base of the Tower domain, that forms a stem of two long alpha-helices and a helix-turn-helix motif, similar to the DNA-binding domains of recombinases and homeodomain transcription factors. Inserts: difference between the occupancy of the lateral chain of wild-type (WT, top) and mutated (bottom) residue at this position.

Figure 2–figure supplement 1: WES metrics for the POI patient

Figure 2–figure supplement 2: Filtering of the variants identified in the POI patient

Figure 2–figure supplement 3: Pathogenicity predictions for the R2842C variant in BRCA2

Figure 2–figure supplement 4: Conservation of the mutated Arg 2842 across species.

BRCA2 loads recombinases on ssDNA: RAD51 in mitotic cells, RAD51 and the meiotic DMC1 in germ cells, indicating a crucial role for BRCA2 in mitotic and meiotic HR (Martinez et al., 2016). Cells defective in RAD51 or BRCA2 are defective in mitotic HR (Lambert and Lopez, 2000; Moynahan et al., 2001) and in mouse, germ cells-specific *Brca2* deletions lead to meiotic impairment and infertility (Miao et al., 2019; Sharan et al., 2004). Therefore, we considered *R2842C-BRCA2* as a very likely causal variant for isolated POI in our patient, although she does not present FA traits. Hence, we investigated the expression of *BRCA2* in human oocytes and the functional impact of the variant on HR in human cells.

BRCA2 is expressed during meiotic prophase I in human fetal ovaries.

In order to support a possible role for BRCA2 in female meiotic HR that would explain this patient's infertility, we verified its expression and localisation in human fetal ovaries. Indeed, *Brca2* mRNA expression was reported in murine oocytes (Sharan et al., 2004) and BRCA2 was described to form recombination nodule-like foci along chromosome axes in human spermatocytes (Chen et al., 1998), but its expression during human female meiosis remained undocumented. Using qRT-PCR on RNA libraries prepared from human ovarian samples at various fetal stages, we detected a predominant expression of *BRCA2* mRNA after 11 weeks post-fertilization, when oocytes enter and progress through meiotic prophase I (Figure 3A).

Immunostaining of human fetal ovarian sections showed that BRCA2 protein was detected mostly in pachytene stage oocytes (Figure 3B). BRCA2 staining appeared as thick threads, likely corresponding to meiotic chromosomes. These results show that BRCA2 is indeed present on chromosomes in fetal human oocytes when meiotic DSB repair occurs.

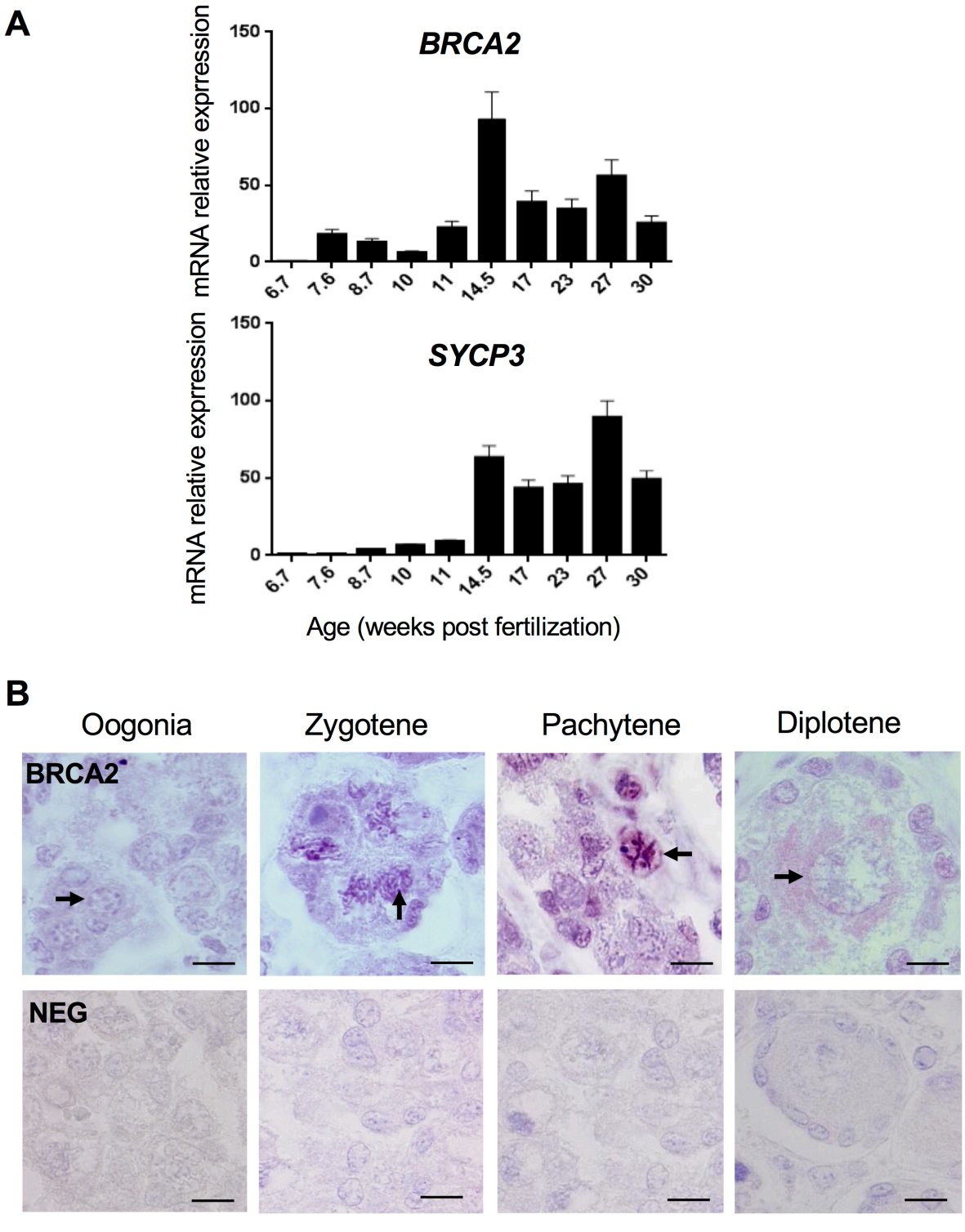

Figure 3: BRCA2 expression in human fetal ovaries. A. *BRCA2* mRNA was quantified by RT-qPCR from total RNA of pooled human fetal ovaries from various developmental stages (above). Beta-actin was used as a reference and expression is provided as percentage of the maximum. Each RNA library was analysed in triplicate and the bar indicates the mean. Quantification of *SYCP3* mRNA is shown at the same stages for comparison (below). **B.** BRCA2 immunostaining (purple) in the cortex of a 24 weeks post fertilization human ovary. Meiotic chromosomes are stained in zygotene and pachytene stage oocytes. No staining is observed when immunohistochemistry is performed in the absence of primary antibody (NEG). Arrowheads point to germ cells at the indicated stage. Scale bar: 10 µm.

R2842C-BRCA2 displays a reduced DSB-induced HR efficiency

Although referenced in the COSMIC database of variants in cancer (COSM23938), *R2842C-BRCA2* is considered as a variant of unknown significance for breast cancer predisposition (VUS, IARC class 3). Attempts to classify BRCA2 VUS in a hamster lung fibroblast cell line showed that this variant displayed a little decrease in HR efficiency, at the limit for inferring pathogenicity (Guidugli et al., 2013). Therefore, the significance of this variant and its classification as a causal mutation for human pathology remained unclear. A previous attempt to classify BRCA2 VUS in a hamster lung fibroblast cell line showed that this variant displayed a little decrease in HR efficiency, at the limit for inferring pathogenicity (Guidugli et al., 2013). Since human and rodent cells differ in their regulation of DSB repair, we analysed the specific impact of R2842C-BRCA2 on HR in human cells. We used the RG37 cell line (Dumay et al., 2006), a human SV40 immortalized fibroblast line bearing the DR-GFP substrate (Pierce et al., 1999) that monitors gene conversion induced by targeted cleavage by the I-SceI meganuclease (Figure 4A). Both the expression of WT-BRCA2 and R2842C-BRCA2 stimulated the efficiency of DSB-induced HR (Figure 4B). We then silenced the endogenous *BRCA2* using a specific siRNA targeting its 3'UTR sequence, and complemented these cells with either the WT or mutated BRCA2 (Figure 4C). As expected, silencing endogenous *BRCA2* decreased HR efficiency, and WT-BRCA2 fully complemented HR efficiency. R2842C-BRCA2, expressed at

similar levels than WT-BRCA2, only partially complemented HR efficiency, to 67 ± 6% compared to WT-BRCA2 (Figure 4B).

These data show that the *R2842C-BRCA2* mutation affects HR efficiency in human cells, but only partially. This significant residual activity could account for the absence of somatic pathology in the patient.

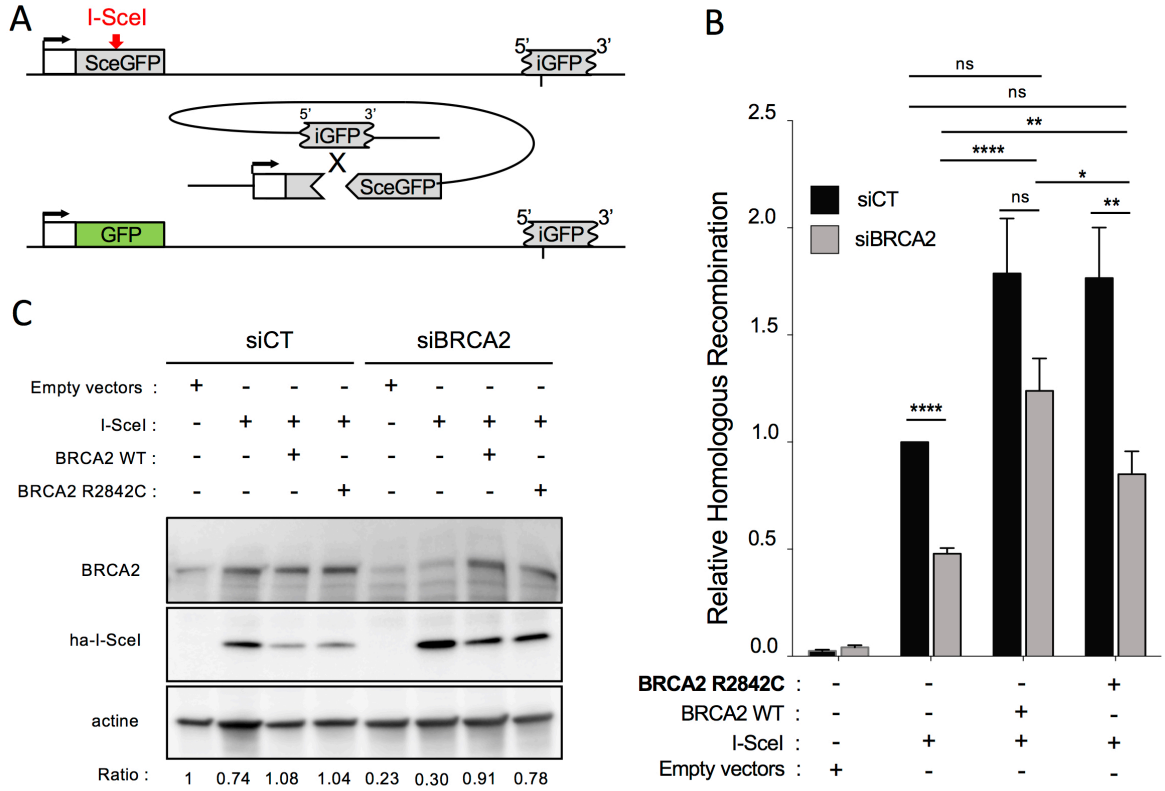

Figure 4: Impact of the *R2842C-BRCA2* mutation on homologous recombination induced by targeted DSB. A. Schematic representation of the DR-GFP substrate for the study of homologous recombination. Two inactive GFP (iGFP and SceGFP) genes are organised into direct repeats. The I-SceI meganuclease generates a targeted DSB cleavage into the substrate (red). HR between the two GFP genes generates a functional GFP. The DR-GFP substrate is stably integrated in the SV40-transformed fibroblasts RG37 cell line, and the relative HR efficiency is quantified as the fraction of GFP-positive cells (i.e with a repaired GFP gene after targeted cleavage), as scored by FACS. **B.** HR efficiency, measured by the fraction of GFP+ cells, in cells expressing the WT or mutated BRCA2 protein (normalised to I-SceI transfected

cells), and transfected either with a control siRNA (siCT) or a siRNA targeting the 3'UTR of endogenous *BRCA2* mRNA (siBRCA2). The values are normalised to the control and represent the average ± SEM (p-values from Mann-Whitney test) for at least 3 independent experiments. **C.** Expression of endogenous BRCA2 and exogenous WT-BRCA2 and R2842C-BRCA2. Twenty micrograms of total proteins extracted from a wild type or R2842C mutant BRCA2-expressing cell line were electroblotted in the presence of endogenous BRCA2 (siCT) or after specific silencing (siBRCA2). For each condition, the expression of I-SceI and BRCA2 and the efficiency of silencing were measured. We used β-actin as a loading control. Below: relative quantification of BRCA2 versus actin by quantification of bands intensity with ImageJ.

Increased chromosomal instability in the patient's cells

Then we studied mitomycin C (MMC)-induced chromosomal breaks in lymphoblastoid cells derived from the patient, her mother, two fertile control women and a FANCD1 patient. In the absence of MMC, few spontaneous breaks were observed in cells from the proposita and the FANCD1 patient (Figure 5A and 5B). Upon exposure to 300 nM MMC, all FANCD1 cells presented breaks, as expected, while the patient's cells exhibited a slight increase of chromosomal breaks, compared to the heterozygous mother's and the WT control cells. Furthermore, at high MMC dose (1000 nM), while breaks in FANCD1 cells were too numerous to be quantified, the patient's cells presented only a modest increase of breaks (Figure 5B). These data show that the patient's cells display levels of chromosomal breaks intermediate between those of WT and FANCD1 cells.

Reduced proliferation rate of the patient's primary fibroblasts

Then we compared the proliferation rate of primary fibroblasts from the POI patient, WT controls and a FANCD1 patient. As expected, the proliferation of FANCD1 cells was markedly affected when compared to that of the WT cells (Figure 5C). Remarkably, the patient's fibroblasts exhibited a moderately reduced proliferation rate, intermediate between the WT and the FANCD1 cells.

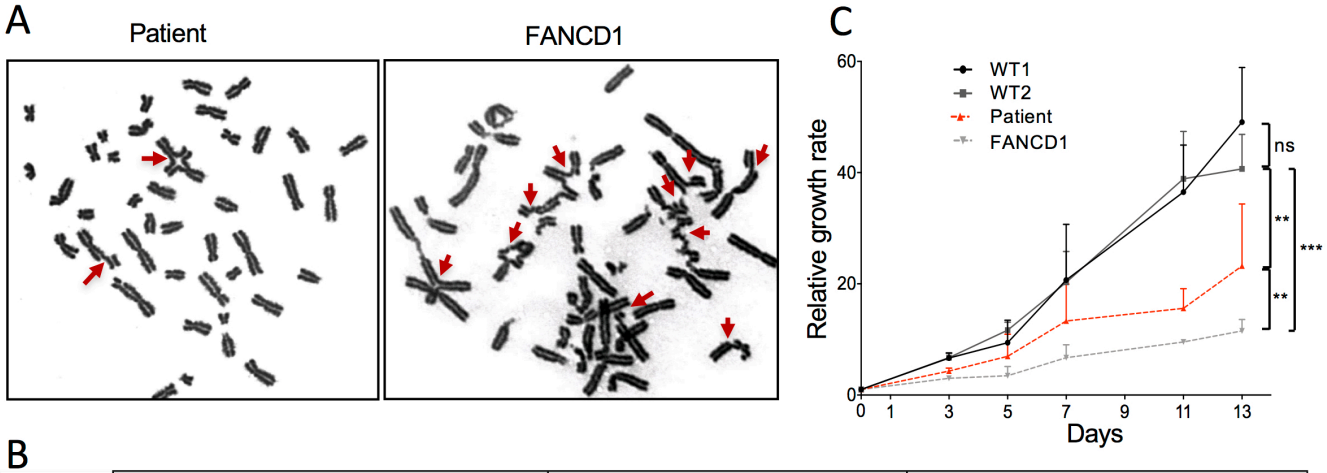

B

	Aberrant metaphases			Breaks/ metaphase			Radial figures		
	Untreated	MMC (300 nM)	MMC (1000 nM)	Untreated	MMC (300 nM)	MMC (1000 nM)	Untreated	MMC (300 nM)	MMC (1000 nM)
Control	0/50 (0%)	1/50 (2%)	3/20 (15%)	0	0.14	0.21	0/50 (0%)	0/50 (0%)	1/20 (5%)
Mother	0/50 (0%)	2/50 (4%)	3/18 (17%)	0	0.2	0.39	0/50 (0%)	1/50 (2%)	1/18 (6%)
Patient	1/50 (2%)	9/50 (18%)	11/25 (44%)	0.02	0.38	1.04	0/50 (0%)	2/50 (4%)	4/25 (16%)
FANCD1	4/50 (8%)	41/41 (100%)	20/20 (100%)	0.08	4.5	high	0/50 (0%)	35/41 (85%)	numerous

Figure 5: Increased chromosomal instability and reduced proliferation rate in the patient's cells. A. Chromosomal breaks analysis of lymphoblastoid cell lines. Metaphases in the patient's and FANCD1 cells in the presence of 300 nM Mitomycin C (MMC). Chromosomal breaks and radial figures are shown (arrows). **B.** Quantification of chromosomal breaks in lymphoblastoid cell lines derived from the patient, the mother, a *FANCD1* patient and a WT control, in the absence or in the presence of MMC. **C.** Reduced proliferation rate of the patient's primary fibroblasts. Cells from the POI patient, two WT controls (WT1 and WT2) and a FANCD1 patient were cultured into 6-wells plates and counted every 2-3 days during thirteen days. The value corresponds to the mean + SEM of at least 3 independent experiments. The statistical significance was calculated from rope comparison of linear regression of growth curves.

Altered radiation-induced RAD51 foci formation in the patient's fibroblasts

The main role for BRCA2 is the loading of the pivotal RAD51 recombinase on damaged DNA, a crucial step for triggering HR. Therefore, we monitored the radiation-induced assembly of

RAD51 foci, which are considered sites of HR initiation events. As expected, FANCD1 cells failed to assemble RAD51 foci (Figure 6A and 6B). The patient's cells showed an intermediate phenotype: indeed, at 6 Gy, they assemble foci with kinetics comparable to WT cells, but the level of the plateau was about two-fold lower than in WT cells (Figure 6B). A dose-response analysis confirmed the complete deficiency in RAD51 foci assembly in FANCD1 cells, at all irradiation doses (Figure 6C and 6D). In the patient's cells, the number of RAD51 foci increased up to 2 Gy similarly to WT cells, but did not further increased at higher doses (Figure 6C, Figure 6D left panel). Consequently, the patient's cells showed lower levels of RAD51 foci at high doses (>2 Gy) when compared to WT cells (Figure 6C, Figure 6D right panel). Together, these data show a dose-dependent sensitivity in the patient's cells, able to process low levels of DNA damage, but failing to assemble RAD51 foci when faced with high levels of damage.

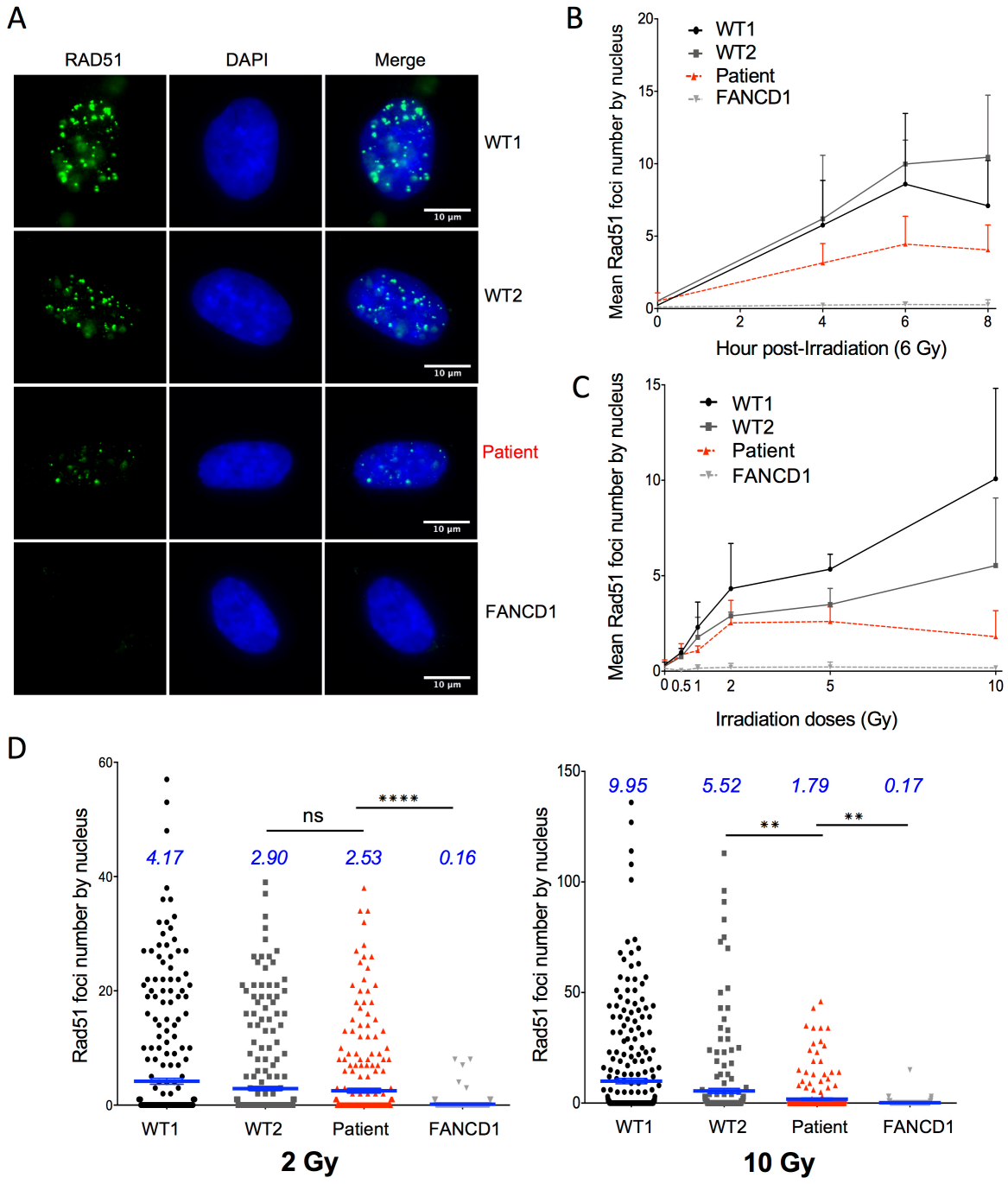

Figure 6: Dose-sensitive alteration of RAD51 foci formation in the patient's cells. A. RAD51 nuclear foci assembly in irradiated primary fibroblasts from the patient, two WT controls and a FANCD1 patient (6 Gy, 6 hours). Fixed and permeabilised cells were probed with an anti-RAD51 antibody. **B.** Kinetics of RAD51 foci assembly (6 Gy) in irradiated primary fibroblasts. **C, D.** Dose response of RAD51 foci assembly (6h post-irradiation) in irradiated primary fibroblasts. **C.** Complete dose response of RAD51 foci per nucleus; **D.** RAD51 foci at low (2 Gy, left panel) and high (10 Gy, right panel) levels of irradiation respectively (medians

are in blue (n=3)). In B and C, the values correspond to the mean + SEM (n=3); p-values (stars) were obtained with Mann-Whitney test.

Figure 6-figure supplement 1: Compilation of WES data for all genes involved in the FA pathway

Bi-allelic mutations in two distinct genes of the FA pathway can be found in a single individual (Singh et al., 2009). In order to rule out that the cellular phenotypes observed in the patient's cells could be due to mild bi-allelic mutations in FA genes other than *BRCA2*, we have analysed the variants found by WES in the 26 other FA genes. The good coverage of each gene, the presence of heterozygous variants (both in coding regions and in UTRS or intronic regions) and unbiased allelic ratios exclude the possibility of having missed a pathogenic variant in another FA gene (Figure 6-figure supplement 1). This analysis supports the fact that the cellular phenotypes observed in the patient's cells are not due to mutations in FA genes other than *BRCA2*. In particular, no variants in *RAD51* could explain the defects in foci assembly detected in the patient's cells.

Discussion

We report here for the first time a *BRCA2* homozygous hypomorphic mutation in a patient with POI, and, remarkably, without cancer nor Fanconi anemia traits in the patient and her family. The mutation is located in the ssDNA-binding domain of BRCA2. We performed a thorough functional study and showed that the R2842C-BRCA2 mutant displays a reduced residual HR activity. Consistently, the patient's cells exhibit a reduced rate of proliferation, a slight increase in MMC-induced chromosomal breaks and a dose-sensitive alteration of radiation-induced assembly of RAD51 foci. However, despite these moderate alterations in somatic cells, the patient did not develop somatic pathology, unlike FANCD1 patients.

Meiotic recombination is a complex and highly regulated process occurring in meiotic prophase I and involving specific meiotic genes such as *DMC1* and *MEIOB* (Crickard et al., 2018; Souquet et al., 2013; Yoshida et al., 1998). While the role and clinical impact of homozygous and heterozygous *BRCA2* variants in mitotic cells is widely studied, the impact of such defects in human germ cells remains less understood because almost all FANCD1 patients die before puberty. However, it was very recently shown in mouse models that oocyte-specific *Brca2* defects lead to meiotic impairment, germ cells depletion and infertility (Miao et al., 2019; Tsui and Crismani, 2019). Here, we show that BRCA2 mRNA and protein are expressed in human fetal ovaries in pachytene stage oocytes, when meiotic HR occurs. Taken together, our data strongly support an actual role of BRCA2 in meiotic HR, and therefore a likely impact of R2842C-BRCA2 reduced activity on this process in our POI patient.

The main role of BRCA2 is the loading of the pivotal recombinase RAD51 on damaged DNA, to allow for repairing DSBs by HR. Using a HR reporter assay and quantification of RAD51 foci in the patient's irradiated somatic cells, we show here that the R2842C-BRCA2 mutant exhibits a reduced DSB-induced HR efficiency, but that RAD51 foci assembly was not affected at low irradiation doses. In addition, the patient's cells displayed a growth rate and levels of chromosomal breaks intermediate between FANCD1 cells and WT cells. This shows that the patient's somatic cells are slightly altered when compared to WT cells, but at a level insufficient to cause somatic pathological consequences. Since R2842C-BRCA2 cells efficiently load RAD51 on low numbers of DNA damage, the residual HR activity of the R2842C-BRCA2 mutant could account for the absence of somatic disorders.

Meiotic recombination in germ cells is initiated by hundreds of DSBs, and crossing-overs (involving HR) are required to produce functional gametes (Zhang et al., 2019). By contrast, somatic DSBs are introduced by accident and such cells are rarely spontaneously confronted to such high levels of simultaneous DSBs. In our functional test, RAD51 foci assembly by the

mutated BRCA2 was significantly decreased at higher doses (>5 Gy) that generate a high number of DSBs (with an estimation of 30 to 40 DSB/Gy/mammalian genome (Ruiz de Almodóvar et al., 1994)). Therefore, the *R2842C-BRCA2* mutation is expected to affect the processing of such a high number of simultaneous meiotic DSBs, explaining the infertility observed in our patient.

Heterozygous BRCA2 mutations increase susceptibility to familial breast and ovarian cancer (Walsh et al., 2011). Such increased susceptibility has not been observed in our patient's family. The efficient loading of RAD51 on low number of DNA damages in the patient's somatic cells could explain the absence of somatic pathologies. Although we cannot rule out the possibility that the patient may develop cancer on the long-term, after triggering by environmental causes, the fact that neither the patient nor her relatives have yet developed other pathologies implies that the *BRCA2* mutation is hypomorphic and retains a residual HR activity, as supported by our functional studies.

Recently, two young sisters presenting a syndromic XX ovarian dysgenesis were reported to carry compound heterozygous C-terminal *BRCA2* truncations. However, in addition to POI, these patients and their family fulfilled the diagnostic criteria of FA: microcephaly, café-au-lait spots, childhood leukemia, and a characteristic severe cellular response to mitomycin in chromosomal breakage tests (over 100 breakages per cells at 150 and 300 nM MMC, 50 times the number observed in control lymphocytes), the hallmark of FA (Auerbach, 2009; Weinberg-Shukron et al., 2018). Therefore, these cases are not similar to our patient that presents only an isolated POI.

In conclusion, we describe and functionally characterize here for the first time a homozygous hypomorphic variant of BRCA2, in a patient with isolated POI without somatic pathology in the patient and her family. The recent implication of DNA repair genes in POI establishes a genetic link between infertility and cancer. As *BRCA2* is a major susceptibility gene for breast

and ovarian cancer, this represents a major ethical issue for the care of these patients. It should change the genetic counselling and pre-test information for patients with isolated POI and their families. Indeed, such counselling should be addressed while keeping in mind a possible defect in major DNA repair genes such as *BRCA2*. More generally, this study has also a wide impact for the understanding of the processes controlling genome plasticity and the consequences of their defects, in somatic and germ cells.

MATERIAL AND METHODS

Ethics statement

The study was approved by all the institutions involved and by the agence de Biomedecine (reference number PFS12-002). Written informed consent was received from participants prior to inclusion in the study.

Whole Exome Sequencing and bioinformatics analysis

WES, reads quality check and mapping was performed by Beckman Coulter Genomics (Danvers, USA). Exon capture was performed using the hsV5UTR kit target enrichment kit. Mapping was performed on the GRCh37.p13 reference genome using the Burrows-Wheeler Alignment tool (BWA) version 0.6.1-r104 with default parameters, and samtools 'Rmdup' was used to remove duplicates. Prior to variant calling, reads were re-aligned around known or suspected indels by the GATK Realigner commands. The samtools version 2.0 'mpileup' command and the bcftools multi-allelic calling model were used for variant calling. Variants were annotated by SnpEff, VEP (Variant Effect Predictor) and dbNSFP 3.5a. Minor Allele Frequencies were manually verified using ExAC (http://exac.broadinstitute.org/), Gnomad (https://gnomad.broadinstitute.org/) and Kaviar (http://db.systemsbiology.net/kaviar/) databases.

387

388 **Sanger Sequencing Analysis**

389 To confirm the presence and segregation of the variant, direct genomic Sanger DNA sequencing
390 of *BRCA2* was performed in the patient and both parents using specific *BRCA2* primers: 5'-
391 GACTACCCTCTCATAGCTCCAG-3' and 5'-GGAAGAAGCAGGGAACACTC-3'

392

393 **Protein modelisation**

394 The 1mje and 1miu structures of BRCA2 were retrieved from PDB databank 1. The 1mje
395 structure was opened in iMol (Piotr Rotkiewicz, "iMol Molecular Visualization Program,"
396 (2007) http://www.pirx.com/iMol) for displaying the proximity of the mutation to the DNA-
397 binding groove in the C-terminal domain of the BRCA2 protein. The human WT and mutated
398 sequence were threaded onto the 1miu structure using RaptorX 2, and the resulting pdb
399 structures were rendered in iMol for displaying the occupancy of lateral chains.

400

401 **Collection of human samples**

402 GM3348 (WT1) and GM3652 (WT2) are wild-type primary human fibroblasts (Coriell institute,
403 Camden, USA). EGF 208_F, noted as FANCD1 cells, are primary fibroblast from a FANCD1
404 patient biopsy (generous gift from Dr. Jean Soulier, Hopital St Louis, Paris). Primary fibroblasts
405 were derived from a skin biopsy of the patient. EBV-immortalized lymphoblastoid cell lines
406 derived from the patient, both parents and two healthy women as control were established at the
407 Banque de cellules, Genopole (Evry, France) using a standard protocol.

408

409 **Collection of human fetal gonads**

Human fetal ovaries were obtained and studied as described (Frydman et al., 2017). Fetal ovaries were harvested from material obtained following legally induced abortions or therapeutic terminations of pregnancies at the Department of Obstetrics and Gynecology at the Antoine Béclère Hospital, Clamart (France). All women provided an informed consent and this study was approved by the Biomedicine Agency (reference number PFS12-002). Fetal age was calculated by measuring the length of limbs and feet according to a developed mathematical model (Evtouchenko et al., 1996). After collection, fetal gonads were stored in RLT RNA lysis buffer (Qiagen, Courtaboeuf, France) for gene expression profiling or fixed for histology and immunostaining. Fetal ovaries from the therapeutic terminations of pregnancies (second and third trimester of pregnancy) had to display normal histological features before being included in the study.

Detection of BRCA2 in human fetal ovaries

Immunohistochemistry was studied as previously described (Poulain et al., 2015). Fetal human ovaries were fixed overnight in 10% neutral formalin (Carlo Erba Reagents, Val de Reuil, Frane) before being dehydrated, embedded in paraffin wax and cut into 5µm sections. After dewaxing and rehydration, antigen retrieval was performed in HIER citrate buffer pH 6 (Zytomed, Diagomics, Blagnac, France) in an autoclave (Retriever 2100, Proteogenix, Mundolsheim, France). Sections were then bathed in distilled water and incubated for 15 min in 3% H2O2 at room temperature. After 30 min in 2.5% normal Horse serum (Vector laboratories, Eurobio, Les Ulis, France), primary antibody diluted in PBS was incubated for 2h at 37°C. The primary antibody used in this study was rabbit polyclonal to human BRCA2 (1:200, Abcam, Paris, France). The primary antibody was revealed using the secondary antibody anti-rabbit IgG (IMPRESS kit, Vector Laboratories, Eurobio). Peroxidase activity was visualized using VIP (Vector laboratories, Eurobio) as a substrate. Sections were counterstained with hematoxylin.

435

436 **Real-time quantitative PCR**

437 In order to measure the expression of multiple genes during human gonadal development, total
438 RNA from fetal ovaries was extracted using the RNeasy Mini Kit (Qiagen Courtaboeuf, France),
439 followed by a reverse transcription and whole transcriptome amplification (Quantitect Whole
440 Transcriptome cDNA Amplification, Qiagen, Courtaboeuf, France). Seventeen ovaries were
441 included for gene expression profiling as previously described (Poulain et al., 2014). Each RNA
442 sample was analysed in triplicate. The 7900HT Fast Real-Time PCR System (Applied
443 Biosystems, Foster City, CA) and SYBR-green labelling were used for quantitative RT-PCR.
444 The comparative ΔΔcycle threshold method was used to determine the relative quantities of
445 mRNA using *ACTB* (ß-actin) mRNA as reference gene for normalization. The sequences of
446 oligonucleotides used with SYBR-green detection were designed with Primer Express Software:
447 ACTB: 5'-TGACCCAGATCATGTTTGAGA-3'; 3'- TACGGCCAGAGGCGTACAGG-5'
448 BRCA2: 5'-AGACTGTACTTCAGGGCCGTACA-3'; 3'-GCTGAGACAGGTGTGGAAAC-5'.
449 SYCP3: 5'-TGCGGTGTGTTTCAGTCAGG-3', 3'-TTTTTCCGGAGGACACCATATT-5'
450

451 **Chromosome breakage studies**

452 Chromosome breakage studies were performed in EBV-immortalized lymphoblastoid cell lines
453 derived from the patient, her mother, a FANCD1 patient and a healthy woman as control. They
454 were studied at the Gustave Roussy Institute (Villejuif, France), following a standard in-house
455 protocol. EBV-immortalized cells were cultured under standard conditions for karyotyping.
456 DNA damage was induced using Mitomycin C (MMC, Sigma) added for 48h. For each sample,
457 three conditions were tested: without MMC to analyze spontaneous damages, and with 300 nM
458 and 1000 nM MMC. Chromosome breakages were scored by an experimented cytogeneticist on
459 at least 20 metaphases.

460

461 **Cell proliferation assay**

462 Primary fibroblasts from the POI patient, two healthy WT controls (GM3348 and GM3562) and
463 a FANCD1 patient were seeded into 6-well cell culture and grown in MEM (Gibco, Life
464 Technologies) supplemented with 20% fetal calf serum (FCS; Lonza Group, Ltd.) and were
465 incubated at 37°C with 5% CO_2. For thirteen days, cells were dissociated from wells with trypsin
466 and counted every 2-3 days using a Z1 Particle Counter (Beckman Coulter).

467

468 **Cell transfection and HR efficiency test**

469 The HR efficiency was assessed in RG37 cell line, derived from SV40-transformed GM639
470 human fibroblasts in which we stably integrated the pDR-GFP gene conversion reporter (Dumay
471 et al., 2006; Pierce et al., 1999). RG37 were cultured in DMEM supplemented with 10% fetal
472 calf serum (FCS) and 2 mM glutamine and were incubated at 37°C with 5% CO_2. For HR
473 efficiency test, The I-SceI meganuclease was expressed by transient transfection of the pCMV-
474 HA-I-SceI expression plasmid (Liang et al., 1998) with Jet-PEI according to the manufacturer's
475 instructions (Polyplus transfection), and cells were incubated for 48 hours. Cells were collected
476 in PBS and 50 mM EDTA, pelleted and fixed with 2% paraformaldehyde for 20 minutes. The
477 percentage of GFP-expressing cells was scored by FACS analysis using a BD Accuri C6 flow
478 cytometer (BD Biosciences).
479 For silencing experiments, 20000 cells were seeded 1 day before transfection with siRNAs,
480 using INTERFERin following the manufacturer's instructions (Polyplus Transfection) with 20
481 nM of one of the following siRNAs: Control (5'-AUGAACGUGAAUUGCUCAA-3'), BRCA2-
482 3 (5'-GCUUCAGUUGCAUAUCUUA-3'). The BRCA2 siRNA targets the 3'UTR of endogenous
483 BRCA2 mRNA. All siRNAs were synthesized by Eurofins (France). Forty-eight hours later, the
484 cells were transfected with the pCMV-HA-I-SceI expression plasmid. At least 3 independent

485 experiments were performed, and HA-I-SceI expression and silencing efficiency were verified
486 by Western blot as described below.
487
488 **Western blotting**
489 Cells were lysed in buffer containing 20 mM Tris HCl (pH 7.5), 1 mM Na_2EDTA, 1 mM EGTA,
490 150 mM NaCl, 1% (w/v) NP40, 1% sodium deoxycholate, 2.5 sodium pyrophosphate, 1 mM β-
491 glycerophosphate, 1 mM NA_3VO_4 and 1 µg/ml leupeptin supplemented with complete mini
492 protease inhibitor (Roche). Denatured proteins (20-40 µg) were electrophoresed in 9% SDS-
493 PAGE gels or NuPAGE™ 3-8% Tris-Acetate Protein Gels (Invitrogen), transferred onto a
494 nitrocellulose membrane and probed with specific antibodies: anti-BRCA2 (1/4000, ab9143,
495 Abcam), anti-Vinculin (1/8000, ab18058 Abcam), and anti-HA (1/1,000, F-7 #sc-7392,
496 SantaCruz). Immunoreactivity was visualized using an enhanced chemiluminescence detection
497 kit (ECL, Pierce). The intensity of the bands was quantified by ImageJ.
498
499 **Irradiation**
500 Cells were exposed to 0.5, 1, 2, 5, 6 or 10 Gy IR 24h after seeding using an X-ray source (1.03
501 Gy/min) (X-RAD 320, Precision X-Ray Inc., North Branford, CT). The cells were fixed with
502 4% paraformaldehyde 2h, 4h, 6h, 8h or 24h after irradiation, and immunofluorescence was
503 performed as described below.
504
505 **Immunofluorescence**
506 Cells were seeded onto slides, then washed with PBS, treated with CSK buffer (100 mM NaCl,
507 300 mM sucrose, 3 mM $MgCl_2$, 10 mM Pipes pH 6.8, 1 mM EGTA, 0.2X Triton, and protease
508 inhibitor cocktail (complete ULTRA Tablets, Roche) and fixed in 2% paraformaldehyde for 15
509 min. The cells were then permeabilized in 0.5% Triton-X 100 for 5 min, saturated with 2% BSA

and 0.05% Tween20 and probed with anti-RAD51 antibody (1/500, PC130, Merck Millipore) for 2 h at 37°C. After 3 washes in PBS-Tween20 (0.05%) at RT, the cells were probed with Alexa-coupled anti-mouse or anti-rabbit secondary antibody (1/1,000, Invitrogen) for 1h at 37°C. After 3 washes, the cells were mounted in DAKO mounting medium containing 300 nM DAPI and visualized using a fluorescence microscope (Zeiss Axio Observer Z1) equipped with an ORCA-ER camera (Hamamatsu). Image processing and foci counting were performed using the ImageJ software.

Statistical Analysis

Statistical analyses were performed using GraphPad Prism 3.0 (GraphPad Software).

Acknowledgements:

We thank Baptiste Fouquet for help in some experiments, Jean Soulier and the "Cellulothèque des hémopathies de l'Hôpital Saint-Louis » for the gift of FANCD1 primary fibroblasts and Alexandra Benachi for fetal ovaries. This study was supported by Université Paris Diderot (SC), Université Paris Sud-Paris Saclay (ED, AH, MM), by the Agence Nationale de Biomedecine (AH, MM) and by Institut Universitaire de France (GL). BSL was supported by the Ligue Nationale contre le cancer "Equipe labellisée 2017", Agence Nationale de la Recherche (ANR-16-CE12-0011-02 and ANR-16-CE18-0012-02), AFM-Téléthon and Institut National du Cancer (INCa-PLBIO18-232).

Authors contributions

MM, GL and BSL designed research studies. ED, AH, ST and SM conducted experiments. SC, ED, AH, GL, BSL and MM acquired and analysed data. MM, SC, BSL, AH and GL wrote the manuscript.

535

536 **Disclosure:**

537 The authors declare no conflict of interest.

REFERENCES

AlAsiri S, Basit S, Wood-Trageser MA, Yatsenko SA, Jeffries EP, Surti U, Ketterer DM, Afzal S, Ramzan K, Faiyaz-Ul Haque M, Jiang H, Trakselis MA, Rajkovic A. 2015. Exome sequencing reveals MCM8 mutation underlies ovarian failure and chromosomal instability. J Clin Invest 125:258–262. doi:10.1172/JCI78473

Auerbach AD. 2009. Fanconi anemia and its diagnosis. Mutat Res 668:4–10. doi:10.1016/j.mrfmmm.2009.01.013

Chen J, Silver DP, Walpita D, Cantor SB, Gazdar AF, Tomlinson G, Couch FJ, Weber BL, Ashley T, Livingston DM, Scully R. 1998. Stable interaction between the products of the BRCA1 and BRCA2 tumor suppressor genes in mitotic and meiotic cells. Mol Cell 2:317–328.

Crickard JB, Kaniecki K, Kwon Y, Sung P, Greene EC. 2018. Meiosis-specific recombinase Dmc1 is a potent inhibitor of the Srs2 antirecombinase. Proc Natl Acad Sci U S A 115:E10041–E10048. doi:10.1073/pnas.1810457115

Dumay A, Laulier C, Bertrand P, Saintigny Y, Lebrun F, Vayssiere JL, Lopez BS. 2006. Bax and Bid, two proapoptotic Bcl-2 family members, inhibit homologous recombination, independently of apoptosis regulation. Oncogene.

Evtouchenko L, Studer L, Spenger C, Dreher E, Seiler RW. 1996. A mathematical model for the estimation of human embryonic and fetal age. Cell Transplant 5:453–464.

Fouquet B, Pawlikowska P, Caburet S, Guigon C, Mäkinen M, Tanner L, Hietala M, Urbanska K, Bellutti L, Legois B, Bessieres B, Gougeon A, Benachi A, Livera G, Rosselli F, Veitia RA, Misrahi M. 2017. A homozygous FANCM mutation underlies a familial case of non-syndromic primary ovarian insufficiency. eLife 6. doi:10.7554/eLife.30490

Frydman N, Poulain M, Arkoun B, Duquenne C, Tourpin S, Messiaen S, Habert R, Rouiller-Fabre V, Benachi A, Livera G. 2017. Human foetal ovary shares meiotic preventing factors with the developing testis. Hum Reprod Oxf Engl 32:631–642. doi:10.1093/humrep/dew343

Guidugli L, Pankratz VS, Singh N, Thompson J, Erding CA, Engel C, Schmutzler R, Domchek S, Nathanson K, Radice P, Singer C, Tonin PN, Lindor NM, Goldgar DE, Couch FJ. 2013. A classification model for BRCA2 DNA binding domain missense variants based on homology-directed repair activity. Cancer Res 73:265–275. doi:10.1158/0008-5472.CAN-12-2081

Hoeijmakers JH. 2009. DNA damage, aging, and cancer. N Engl J Med.

Huhtaniemi I, Hovatta O, La Marca A, Livera G, Monniaux D, Persani L, Heddar A, Jarzabek K, Laisk-Podar T, Salumets A, Tapanainen JS, Veitia RA, Visser JA, Wieacker P, Wolczynski S, Misrahi M. 2018. Advances in the Molecular Pathophysiology, Genetics, and Treatment of Primary Ovarian Insufficiency. Trends Endocrinol Metab TEM 29:400–419. doi:10.1016/j.tem.2018.03.010

Lambert S, Lopez BS. 2000. Characterization of mammalian RAD51 double strand break repair using non-lethal dominant-negative forms. EMBO J 19:3090–3099. doi:10.1093/emboj/19.12.3090

577 Liang F, Han M, Romanienko PJ, Jasin M. 1998. Homology-directed repair is a major double-
578 strand break repair pathway in mammalian cells. Proc Natl Acad Sci U A.

579 Ludwig T, Chapman DL, Papaioannou VE, Efstratiadis A. 1997. Targeted mutations of breast
580 cancer susceptibility gene homologs in mice: lethal phenotypes of Brca1, Brca2, Brca1/Brca2,
581 Brca1/p53, and Brca2/p53 nullizygous embryos. Genes Dev 11:1226–1241.

582 Martinez JS, von Nicolai C, Kim T, Ehlén Å, Mazin AV, Kowalczykowski SC, Carreira A.
583 2016. BRCA2 regulates DMC1-mediated recombination through the BRC repeats. Proc Natl
584 Acad Sci U S A 113:3515–3520. doi:10.1073/pnas.1601691113

585 Meyer S, Tischkowitz M, Chandler K, Gillespie A, Birch JM, Evans DG. 2014. Fanconi
586 anaemia, BRCA2 mutations and childhood cancer: a developmental perspective from clinical
587 and epidemiological observations with implications for genetic counselling. J Med Genet
588 51:71–75. doi:10.1136/jmedgenet-2013-101642

589 Miao Y, Wang P, Xie B, Yang M, Li S, Cui Z, Fan Y, Li M, Xiong B. 2019. BRCA2 deficiency
590 is a potential driver for human primary ovarian insufficiency. Cell Death Dis 10:474.
591 doi:10.1038/s41419-019-1720-0

592 Moynahan ME, Pierce AJ, Jasin M. 2001. BRCA2 is required for homology-directed repair of
593 chromosomal breaks. Mol Cell 7:263–272.

594 Pierce AJ, Johnson RD, Thompson LH, Jasin M. 1999. XRCC3 promotes homology-directed
595 repair of DNA damage in mammalian cells. Genes Dev 13:2633–2638.

596 Poulain M, Frydman N, Tourpin S, Muczynski V, Souquet B, Benachi A, Habert R, Rouiller-
597 Fabre V, Livera G. 2015. Involvement of doublesex and mab-3-related transcription factors
598 in human female germ cell development demonstrated by xenograft and interference RNA
599 strategies. Mol Hum Reprod 21:615. doi:10.1093/molehr/gav029

600 Ruiz de Almodóvar JM, Steel GG, Whitaker SJ, McMillan TJ. 1994. A comparison of methods
601 for calculating DNA double-strand break induction frequency in mammalian cells by pulsed-
602 field gel electrophoresis. Int J Radiat Biol 65:641–649.

603 Sharan SK, Morimatsu M, Albrecht U, Lim DS, Regel E, Dinh C, Sands A, Eichele G, Hasty
604 P, Bradley A. 1997. Embryonic lethality and radiation hypersensitivity mediated by Rad51 in
605 mice lacking Brca2. Nature 386:804–810. doi:10.1038/386804a0

606 Sharan SK, Pyle A, Coppola V, Babus J, Swaminathan S, Benedict J, Swing D, Martin BK,
607 Tessarollo L, Evans JP, Flaws JA, Handel MA. 2004. BRCA2 deficiency in mice leads to
608 meiotic impairment and infertility. Dev Camb Engl 131:131–142. doi:10.1242/dev.00888

609 Singh TR, Bakker ST, Agarwal S, Jansen M, Grassman E, Godthelp BC, Ali AM, Du C,
610 Rooimans MA, Fan Q, Wahengbam K, Steltenpool J, Andreassen PR, Williams DA, Joenje
611 H, de Winter JP, Meetei AR. 2009. Impaired FANCD2 monoubiquitination and
612 hypersensitivity to camptothecin uniquely characterize Fanconi anemia complementation
613 group M. Blood 114:174–180. doi:10.1182/blood-2009-02-207811

614 Souquet B, Abby E, Hervé R, Finsterbusch F, Tourpin S, Le Bouffant R, Duquenne C, Messiaen
615 S, Martini E, Bernardino-Sgherri J, Toth A, Habert R, Livera G. 2013. MEIOB targets single-

616 strand DNA and is necessary for meiotic recombination. PLoS Genet 9:e1003784.
617 doi:10.1371/journal.pgen.1003784

618 Tsui V, Crismani W. 2019. The Fanconi Anemia Pathway and Fertility. Trends Genet TIG
619 35:199–214. doi:10.1016/j.tig.2018.12.007

620 Tsuzuki T, Fujii Y, Sakumi K, Tominaga Y, Nakao K, Sekiguchi M, Matsushiro A, Yoshimura
621 Y, MoritaT null. 1996. Targeted disruption of the Rad51 gene leads to lethality in embryonic
622 mice. Proc Natl Acad Sci U S A 93:6236–6240.

623 Walsh T, Casadei S, Lee MK, Pennil CC, Nord AS, Thornton AM, Roeb W, Agnew KJ, Stray
624 SM, Wickramanayake A, Norquist B, Pennington KP, Garcia RL, King M-C, Swisher EM.
625 2011. Mutations in 12 genes for inherited ovarian, fallopian tube, and peritoneal carcinoma
626 identified by massively parallel sequencing. Proc Natl Acad Sci U S A 108:18032–18037.
627 doi:10.1073/pnas.1115052108

628 Weinberg-Shukron A, Rachmiel M, Renbaum P, Gulsuner S, Walsh T, Lobel O, Dreifuss A,
629 Ben-Moshe A, Zeligson S, Segel R, Shore T, Kalifa R, Goldberg M, King M-C, Gerlitz O,
630 Levy-Lahad E, Zangen D. 2018. Essential Role of BRCA2 in Ovarian Development and
631 Function. N Engl J Med 379:1042–1049. doi:10.1056/NEJMoa1800024

632 Wood-Trageser MA, Gurbuz F, Yatsenko SA, Jeffries EP, Kotan LD, Surti U, Ketterer DM,
633 Matic J, Chipkin J, Jiang H, Trakselis MA, Topaloglu AK, Rajkovic A. 2014. MCM9
634 mutations are associated with ovarian failure, short stature, and chromosomal instability. Am
635 J Hum Genet 95:754–762. doi:10.1016/j.ajhg.2014.11.002

636 Yang H, Jeffrey PD, Miller J, Kinnucan E, Sun Y, Thoma NH, Zheng N, Chen P-L, Lee W-H,
637 Pavletich NP. 2002. BRCA2 function in DNA binding and recombination from a BRCA2-
638 DSS1-ssDNA structure. Science 297:1837–1848. doi:10.1126/science.297.5588.1837

639 Yoshida K, Kondoh G, Matsuda Y, Habu T, Nishimune Y, Morita T. 1998. The mouse RecA-
640 like gene Dmc1 is required for homologous chromosome synapsis during meiosis. Mol Cell
641 1:707–718.

642 Zhang J, Fujiwara Y, Yamamoto S, Shibuya H. 2019. A meiosis-specific BRCA2 binding
643 protein recruits recombinases to DNA double-strand breaks to ensure homologous
644 recombination. Nat Commun 10:722. doi:10.1038/s41467-019-08676-2

645

FIGURES SUPPLEMENTS:

Figure 2–figure supplement 1.

Whole Exome Sequencing and mapping data for the patient with POI

Generated reads	% GC	Mapped Reads	Properly Mapped Reads	Reads on Target	Forward Strand	Reverse Strand	Strand Bias	Mapped Pairs	Proper Pairs	Singletons
52,025,212	48%	51,991,410	99.90%	71.20%	50%	50%	0%	99.90%	99%	0%

Read Pairs	Average Coverage	>5X	>10X	Picard duplicates	Samtools duplicates	Median Coverage after removing duplicates
25,967,308	51X	69.9%	67.9%	7.2%	7.2%	42.6X

(Back to main text)

Figure 2–figure supplement 2.

Filtering of the variants identified by Whole Exome Sequencing in the POI patient

Variants called in	Patient
Total	**219475**
SNPs	193442
Indels	26033

Variant filters	# of variants
Minimum depth at variant >= 5	86422
Homozygous	44483
in protein coding gene	21693
in coding sequence or splice	7588
with impact on CDS	4521
not Homozygous in fertile controls	1141
MAF < 1% in GnomAD	10
with pathogenicity predictions	5
with coherent functional information	2

Details about the second variant are provided in the Supplementary Information.

(Back to main text)

Figure 2–figure supplement 3.

Pathogenicity predictions for the R2842C variant in *BRCA2*

Software	Score for the variant	Pathogenicity threshold	Pathogenicity prediction
SIFT	0	< 0.05	Deleterious
PolyPhen 2	1	> 0.8	Damaging
M-CAP	0.502	> 0.025	Possibly pathogenic
FATHMM-MKL	0.9452	> 0.5	Deleterious
LRT	0.000003	Score is a p-value	Deleterious
MutationTaster	1	0.5	Disease-causing
MutationAssessor	2.67	> 0.65	Medium
FATHMM	-1.88	< -1.5	Deleterious
FATHMM-MKL coding	0.94518	0.5 (default) 0.80 (stringent)	Deleterious
PROVEAN	-2.38	-2.28	Neutral
MetaSVM	0.6583	0	Deleterious
MetaLR	0.7556	0.5	Deleterious
REVEL	0.843	0.5 (default) 0.75 (stringent)	Pathogenic
DANN	0.9990224	0.96	Damaging
CADD	8.14	1.75	Damaging
GERP++ RS	5.1	> 4.4	Highly conserved
phyloP100way_vertebrate	4.63	> 1.6	Highly conserved

(Back to main text)

Figure 2–figure supplement 4.

Conservation of the mutated BRCA2 Arg 2842 aminoacid across species.

Human (*Homo sapiens*)	MEKTSSGLYIF**R**NEREEEKEAAKYVEAQQKRLEALFTKIQEE
Mouse (*Mus musculus*)	VEKTVSGLYIF**R**SEREEEKEALRFAEAQQKKLEALFTKVHTE
Naked mole-rat, female (*H. glaber*)	MEKTSSGLYIF**R**NEREEEKEAAKHAEAQQKKLEVLFTKIQGQ
Platypus (*Ornithorhynchus anatinus*)	MEKTHTGSYVF**R**NERAEEKEASKHAESQQKKLEALYAKIQDD
Chicken (*Gallus gallus*)	MEKTSAGSYVF**R**NSRAEEREAAKHAEDQQKKLEALFAKIQAE
Anole lizard (*Anolis carolinensis*)	MEKTSTGSYMF**R**NCRAEEREAAKHAENKQKTLEALLANIQAE
Chinese softshell turtle (*Pelodiscus sinensis*)	VEKMPTGSYVF**R**NGRAEEREAAKHAENRQKHLEALFSQIQME
Xenopus (*Xenopus tropicalis*)	MEKMANGLYVF**R**NDRAEEREAEKHSANQQKKLEMLFSKIQAE
Tetraodon (*Tetraodon nigroviridis*)	MERKPEGGTVF**R**SGRAEEKEARRYNVHKEKAMEILFDKIQAE
Coelacanth (*Latimeria chalumnae*)	MEKKSDGIFVF**R**NDRAEEREAQRQVENQQRKMESLFAKIQTE
Purple sea urchin (*S. purpuratus*)	MEKLPEGGSVF**R**NAKEEAKAAALHAGRKQNKMEQLFTQIQKQ
Stony coral (*Orbicella faveolata*)	MEKMSDGTNVF**R**NSRLEEREAKKFEADRQKRREKLFLKIQEE
Pacific oyster (*Crassostrea gigas*)	MEKLPDGGSVF**R**TAQAEEKFSQLYQKQQQDAMESLYRKLEKD
Honey bee (*Apis mellifera*)	HEKTSTGESIF**R**NIRCEEKANIIYEKKCRSMIETFYAKAEKY
Florida carpenter ant (*Camponotus floridanus*)	HEKTASGDSIV**R**NAKCEEKAQSTYEQQCLSKIETFYANAEKD
Nematode (*Trichinella spiralis*)	LEKYADGRSVM**R**NERCEEQISLRFAEEVDHLMEKMLERVVND
Thale cress (*Arabidopsis thaliana*)	KERLGEKKSIV**R**SERIE----SRIIQLHNQRRSALVEGIMCE
Mayze (*Zea Mays*)	RERLPDGRFVV**R**SERMERKALELYHQRVSKITEDILFEQQEN
Basidiomycete (*Ustilago maydis 521*)	VDVDKSNAGAP**R**GEQEEAEQREAWLQRREDAMQQLELEAEAE

The sequence of the 42 aa of the BRCA2 Tower domain is shown in 19 different species across a wide evolutionary range. The strict conservation of the arginine residue supports its functional importance.

(Back to main text)

Figure 6-figure supplement 1.

Whole Exome Sequencing data from the POI patient for all genes included in the FANC pathway, with the exception of BRCA2, to exclude a potential causative variant in all these genes.

Gene name	Alias	Mean Depth in targeted exons (1)	Nb variants in gene (2)	Htz variants (3)	Mean depth at variant positions (4)	Mean ratio for htz allelic reads (5)	Presence of htz variants (6)					Nbr of rare coding variants (7)	
							upstream	5'UTR	deep intronic	3'UTR	downstream	Hmz	and pathogenic
FANCA		65.6	35	31	39.4	1.07	yes	no	yes	yes	yes	0	0
FANCB		63.9	4	4	15.3	1.30	no	yes	yes	no	yes	0	0
FANCC		39.9	0 in this individual										
FANCD1	*BRCA2*	65.9	13	0	36.8	-	-	-	-	-	-	**1**	**1**
FANCD2		73.9	8	7	22.5	0.55	yes	no	yes	no	no	0	0
FANCE		54.2	7	3	30.7	0.85	no	yes	yes	no	no	0	0
FANCF		49.4	2	2	17	0.89	no	no	no	yes	no	0	0
FANCG		73.8	2	2	97.5	0.92	yes	no	yes	no	no	0	0
FANCI		93.6	2	0	33.5	-	-	-	-	-	-	0	0
FANCJ	*BRIP1*	79.7	7	4	42.4	0.95	no	no	yes	yes	no	0	0
FANCL		63.4	2	2	39.5	0.75	no	no	yes	no	no	0	0
FANCM		55.6	0 in this individual										
FANCN	*PALB2*	97.8	0 in this individual										
FANCO	*RAD51C*	70.4	0 in this individual										
FANCP	*SLX4*	61.3	1	1	50	1.13	no	no	no	no	no	0	0
FANCQ	*ERCC4*	78.2	2	0	17	-	-	-	-	-	-	0	0
FANCR	*RAD51*	58.5	32	20	30.2	0.94	yes	no	yes	no	no	0	0
FANCS	*BRCA1*	90.1	16	13	63.4	0.97	yes	no	yes	no	yes	0	0
FANCT	*UBE2T*	81.0	1	0	26	-	-	-	-	-	-	0	0
FANCU	*XRCC2*	40.2	0 in this individual										
FANCV	*MAD2L2*	51.9	4	2	51	1.01	no	no	no	no	yes	0	0
FAAP100	*C17orf70*	47.7	3	1	31	2.00	no	no	no	no	yes	0	0
FAAP24	*C19orf40*	83.6	2	0	29.5	-	-	-	-	-	-	0	0
FAAP20	*C1orf86*	47.2	5	3	32	1.34	no	no	no	no	yes	0	0
FAAP16	*APITD1*	32.8	0 in this individual										
FAAP10	*STRA13*	34.9	0 in this individual										
FAN1		85.5	6	6	36.3	1.01	yes	no	no	yes	no	0	0
	mean	**64.4**	**154**	**101**	**37.1**	**1.05**							

(1) For each gene, the mean depth per probe was averaged over all exons of the gene. The good coverage for all genes excludes the possibility of not detecting a causative variant in other FANC genes.

(2) Total number of upstream, downstream, 5' & 3' UTRs, intronic, synonymous, splice site, missense, frameshift and stop variants in each gene.

(3) The presence of heterozygous variants in a gene excludes the possibility of hemizygosity.

(4) For each gene, the mean depth at variant position was averaged for all variants. The good coverage of variant positions warrants a correct genotyping.

(5) The ratio between the number of reads for each allele was averaged for all heterozygous variants. A ratio close to 1 indicates no biais and argues against a possible deletion of the gene.

(6) The presence of heterozygous variants in the various genic portions argues against the possibility of partial deletions.

(7) Among the 154 variants detected in the genes included in the FANC pathway, only the variant found in BRCA2 is homozygous in the patient, is rare (below 1% in GnomAD database) and predicted as pathogenic.

(Back to main text)

693 **Supplementary Information**

694

695 **Variant analysis in the patient with POI**

696 Variants were annotated by SnpEff and VEP and were filtered on the basis of their
697 homozygosity in the patient, their absence in unrelated fertile in-house controls and a minor
698 allele frequency (MAF) below 0.01 in all available databases. Further filtering on available
699 functional data for a possible role in fertility yielded only two plausible candidate variants. The
700 first variant was a missense rs539695846 in *ARGHEF7*. This gene lies about 250 kb away from
701 one of the 6 loci identified by genome-wide association study as influencing age at natural
702 menopause (Stolk et al., 2009). ARHGEF7 is expressed ubiquitously with a maximum in the
703 brain, and encodes a cytoplasmic Rho guanine nucleotide exchange factor that plays a role in
704 cell proliferation, in particular through phosphorylation of FOXO3a (Chahdi and Sorokin,
705 2008). As *FOXO3a* knockout mice are infertile due to early depletion of the follicle pool
706 (Castrillon et al., 2003), this regulation could be the basis for a possible role of *ARHGEF7* in
707 the age of menopause. However, a recent study showed no association between the
708 polymorphism besides *ARHGEF7* and AMH levels, a reliable marker of ovarian reserve, in
709 childhood cancer survivors (van Dorp et al., 2013) which lessens the interest of this gene in
710 fertility.
711 The second variant was the *BRCA2* missense rs80359104 characterized in this study.
712

713 **Targeted Next Generation Study in the mother**

714 The patient's mother had delayed conception followed by secondary amenorrhea at the age of
715 33 years, not investigated in Turkey. Her amenorrhea, reflecting either a central or peripherical
716 hypogonadism, could be explained in part by obesity, known to contribute to ovulatory
717 dysfunction and amenorrhea (Mircea et al., 2007). Thus, we performed a targeted next

718 generation sequencing (NGS) to eliminate other genetic cause that might explain the potential
719 precocious menopause in the mother. We obtained an average of 1 Gb of sequences with more
720 than 98% of mappable reads and a mean depth of 150x. Nearly 96% of bases were covered to
721 a minimum depth of 20x and more than 95% of the read bases had a Qscore of above 30. A
722 total of four hundred and thirty-seven (437) variants were detected. Twenty variants have a
723 frequency lower than 2% according to the ExAC base. Six false positive variants were ruled
724 out with a careful examination of the corresponding BAMs using IGV. Of the 14 remaining
725 variants, 8 are intronic variants with no predicted effect on splicing. Of the 6 exonic variants,
726 one is a synonymous variant without impact on splicing. Of the remaining five exonic variants,
727 4 are predicted to be benign by the M-CAP prediction software (Table S1). The only remaining
728 variant was the *BRCA2* missense mutation detected in the propositus (our patient, Figure 1,
729 V2), *BRCA2*: c. c.8524C>T; p. Arg2842Cys.
730 *BRCA2* heterozygous mutations were associated with lower AMH levels, reflecting the ovarian
731 reserve (Daum et al., 2018). We cannot exclude that the heterozygous *R2842C-BRCA2*
732 mutation could have an impact on the mother's ovarian reserve in addition to environmental
733 factors.
734

735 **Table S1. Rare Variants detected by Targeted Next Generation Sequencing in the mother**

CHR	POS	REF	ALT	AF	Gene	Exon	cDNA	Protein	GnomAD Genome	GnomAD Exome	Kaviar	ACMG	M-CAP
chr13	**32945129**	**C**	**T**	**0.500**	**BRCA2 (NM_000059.3)**	**exon20**	**c.8524C>T**	**p.Arg2842Cys**	**3.24e-05**	**8.14e-06**	**.**	**Pathogenic Supporting**	**Possibly pathogenic**
chr5	140071240	C	G	0.500	HARS2 (NM_012208.3)	exon1	c.7C>G	p.Leu3Val	0.00352	0.00291	0.000643	VUS	Likely benign
chr12	53818988	T	G	0.500	AMHR2 (NM_020547.2)	exon4	c.464T>G	p.Phe155Cys	.	.	.	VUS	Likely benign
chr22	31867903	C	T	0.500	EIF4ENIF1 (NM_019843.3)	exon3	c.97G>A	p.Glu33Lys	0.00452	0.00378	0.0038	Pathogenic Supporting	Likely benign
chr8	31015010	A	G	0.500	WRN (NM_000553.4)	exon33	c.3946A>G	p.Ile1316Val	.	0.000134	0.000161	VUS	Likely benign

736

737 * VUS: Variant of unknown significance

738 **Supplemental References**

739 Castrillon DH, Miao L, Kollipara R, Horner JW, DePinho RA. 2003. Suppression of ovarian
740 follicle activation in mice by the transcription factor Foxo3a. *Science* **301**:215–218.
741 doi:10.1126/science.1086336

742 Chahdi A, Sorokin A. 2008. Endothelin-1 couples betaPix to p66Shc: role of betaPix in cell
743 proliferation through FOXO3a phosphorylation and p27kip1 down-regulation independently
744 of Akt. *Mol Biol Cell* **19**:2609–2619. doi:10.1091/mbc.e07-05-0424

745 Daum H, Peretz T, Laufer N. 2018. BRCA mutations and reproduction. *Fertil Steril* **109**:33–
746 38. doi:10.1016/j.fertnstert.2017.12.004

747 Mircea CN, Lujan ME, Pierson RA. 2007. Metabolic fuel and clinical implications for female
748 reproduction. *J Obstet Gynaecol Can JOGC J Obstet Gynecol Can JOGC* **29**:887–902.
749 doi:10.1016/S1701-2163(16)32661-5

750 Stolk L, Zhai G, van Meurs JBJ, Verbiest MMPJ, Visser JA, Estrada K, Rivadeneira F,
751 Williams FM, Cherkas L, Deloukas P, Soranzo N, de Keyzer JJ, Pop VJM, Lips P, Lebrun
752 CEI, van der Schouw YT, Grobbee DE, Witteman J, Hofman A, Pols HAP, Laven JSE,
753 Spector TD, Uitterlinden AG. 2009. Loci at chromosomes 13, 19 and 20 influence age at
754 natural menopause. *Nat Genet* **41**:645–647. doi:10.1038/ng.387

755 van Dorp W, van den Heuvel-Eibrink MM, Stolk L, Pieters R, Uitterlinden AG, Visser JA,
756 Laven JSE. 2013. Genetic variation may modify ovarian reserve in female childhood cancer
757 survivors. *Hum Reprod Oxf Engl* **28**:1069–1076. doi:10.1093/humrep/des472

758